Scientia Iranica B (2019) 26(5), 2854–2864

Sharif University of Technology
Scientia Iranica
Transactions B: Mechanical Engineering
http://scientiairanica.sharif.edu

Dynamic behavior of worn wheels in a track containing several sharp curves based on field data measurements and simulation

S.M. Salehi[a], G.H. Farrahi[*], and S. Sohrabpour

School of Mechanical Engineering, Sharif University of Technology, Tehran, Iran.

Received 8 April 2018; received in revised form 28 May 2018; accepted 18 June 2018

KEYWORDS
Dynamic simulation;
Sharp curves;
Field data measurement;
Wear index;
Derailment ratio;
Wheel flange wear.

Abstract. A study of the wheel and rail wear phenomenon can provide a chance for the optimal use of wheel profile, which results in cost efficiency, dynamic stability, travel comfort, and safety to prevent the derailment, especially in curves. In this paper, the experimental data are recorded based on the field measurements for worn wheels of a passenger wagon in the "Southern line" of Iran's railway system and are combined with the dynamic simulations to study the effects of severe wheel flange wear on the dynamics of wagon. The results show that the amount of wheel wear (especially the wheel flange) directly impacts the dynamic behavior of the wagon in curves. In addition, based on the history of wear index and the peak derailment ratio, the appropriate range of the wheel flange thickness required to repair or replace the worn wheels is suggested to be 25 to 27 mm.

1. Introduction

A study of the wheel and rail wear phenomenon can facilitate the optimal use of wheel profile that results in cost efficiency, dynamic stability, travel comfort, and safety to prevent the derailment, especially in curves, and to determine more efficient maintenance schedules for tracks and wagons [1]. Furthermore, wheels' flange wear is a major factor in the maintenance costs associated with railways consisting of several sharp curves, and they should be minimized in order to enhance the competitiveness in the business of the transportation [2]. Although rail/wheel lubrication considerably decreases the wear rate of both elements, wear is still considerably great under heavy haul rail-road conditions in steep curves and when the lubricant film is worn out [3,4].

In the contact of wheel/rail, particularly in sharp curves, the wheel flange is subject to intensive wear [5]. The risk of severe or catastrophic wear resulting from the train's high speed and axle loads increases due to the form change of the wheel-rail contacts in sharp curves, causing wagon lifting and, hence, its derailment [6]. The derailment processes discussed here occur only due to the loss of lateral constraints of the interactions of the rail and wheels. Therefore, any state decreasing the lateral guidance of rail could increase the derailment probability.

Historically, the subject of rail/wheel interaction has been the focus of attention since 1847 when a British commission was appointed to study dynamic effects on railway bridges [7]. The wheel/rail wear has also been extensively studied previously, and the important experimental research pieces were reviewed by Lewis and Olofsson [8], Sheinman [9], and Wang et al. [10], etc. Some of the experimental studies were either conducted through laboratory tests [11-

*. *Corresponding author. Tel.: +98 21 66165533; Fax: +98 21 66000021*
E-mail addresses: s_m_salehi@mehr.sharif.ir (S.M. Salehi); farrahi@sharif.edu (G.H. Farrahi); saeed@sharif.ir (S. Sohrabpour)

doi: 10.24200/sci.2018.50749.1849

15], simulations [16-20], or experience and measurements on in-service vehicles on tracks (field experiments) [13,19,21,22]. The difficulties and expenses involved in the field experiments have forced researchers to use the laboratory tests and simulations, whenever possible [6].

Since the 1970s, researchers have been conducting the numerical simulations of the dynamic behavior of rail vehicles and the interaction between wheels and rail. Quite often, they have become interested in modeling the dynamics of a car trailer with nonlinear component behavior [23]. Some of the earlier software programs developed include Vampire developed by British Rail, Medyna by Deutsche Luft und Raumfahrt, and Nucars in the USA [24]. Recently, general-purpose software programs required for dynamic simulations of multi-body systems such as Gensys, Adams/Rail, Simpack, Dads, Nucars, and Vampire have included features that enable efficient dynamic simulations of wagons and wheel/rail interaction [25], some of which have been benchmarked [26]. By applying the engineering software programs, the dynamics of the rail and the wagon are often classified as two relatively independent problems by assuming the rail as (1) a rigid support or (2) an elastic foundation [27]. By each assumption in the software, the longitudinal, lateral, and vertical dynamics of a moving train or wagon are examined. However, the rail dynamics is also investigated based on two assumptions: (1) the simplified beams on the elastic foundation approach [28] or (2) the Finite Element Model (FEM) of railway system [16,29]. Furthermore, these rail models have almost been assumed to be excited by (1) a single wheel or (2) a single bogie with two wheelsets rolling on the rail [27]. The software used for vehicle motion simulations is normally concerned with the orientation of each wheel relative to the rail, the contact point between wheel tread and rail head, and the contact forces that are caused by the dynamic interaction [30].

In this paper, the experimental data have been recorded from the field measurements of the worn wheel of a passenger wagon in the "Southern line" of Iran's railway system and are combined with the dynamic simulations to study the parameters such as wear index and derailment ratio based on standards UIC510-2, UIC60, and UIC703. In addition, two parameters called wear index and derailment ratio are studied based on the mutual forces of wheel and rail originating from the wagon loads (loads on the wheels from the wagon) and the curves (changes in the wheels' loads due to the track's shape). Here, a model of the wagon with 66 degrees of freedom is considered using the standard UIC518. The dynamic simulation software is utilized to model the wagon and tracks and analyze the effects of wheels' wear on the dynamic behavior of the wagon. This study can suggest strategies, including efficient maintenance strategies, required to examine the safety of the wheel based on the derailment forces.

2. Materials and methods

In this work, dynamic simulations are performed on the wheel and rail models with the same specifications, materials, and mechanical properties according to UIC standards (Table 1). The wear in wheel profiles on the rail wheel of the train traveling between two points has been measured experimentally, where the path contains several sharp curves. The numerical simulations to calculate the dynamic parameters of the train have been performed by considering the experimentally obtained data of the worn profiles of wheels, which highly increase the accuracy of the analysis that may not be achieved simply by a complete simulation process. However, the limitations of empirical work, practical problems, and high costs prevent a complete experimental study. The dynamic analysis is also carried out by appropriate software in such studies. The measurements are recorded on the standard wheel and rail profiles through the travel time.

2.1. Experimental data

2.1.1. The field data measurement path

Experimental data from the field measurements of the wheel profiles are obtained through the traveling of the train in one of the five major rail lines of Iran, i.e., the "Southern line" [31]. This line is very important for passenger and freight transportation from Iran's capital, Tehran, to the three important international transit ports of Iran, i.e., "Imam Khomeini", "Mahshahr", and "Khorramshahr". This line is widely known for the number of sharp curves, leading to a high rate of wheel flange wear.

2.1.2. Measuring instrument and recording procedure

The laser view instrument is used for an automatic measurement of the wheel profiles' parameters. The measurements are performed on a real scale and in-

Table 1. Wheel steel specifications according to UIC 812-3 [39].

Steel category	Carbon content (%)	Yield strength (N/mm^2)	Tensile strength (N/mm^2)	Elongation (%)	Notch impact energy (J)
R7 T,E	≤ 0.52	≥ 520	820	≥ 14	≥ 15

service conditions [31]. The geometry of the worn wheel profiles and the wheel parameters such as flange thickness (Sd) are recorded through each round trip of the train until the flange thickness of the worn wheel reaches the limit of 22 mm (the limit in the standard UIC-510-2 [32] for the detachment of the wagon). The least squares method is utilized as a curve fitting tool in MATLAB software to express the mathematical relationship between the flange thickness (Sd) parameter and the traveled distance of the wagon.

2.2. Modeling and simulation procedure

2.2.1. The characteristics of the test path

The dynamic simulations are carried out by the dynamic simulation software. Part of the path with the highest report of wheel/rail wear including a curve with the shortest radius of curvature within the path is chosen for the purpose of the simulation. The test path is created considering the conditions defined in the standards UIC518 and UIC703 from the real parameters of the Southern line of Iran's railway system with a length of 600 m. According to the standards, the path contains the following parts:

- A straight line with a length of 100 m;
- An interface curve with a length of 50 m;
- A curve with a radius of 220 m and a length of 300 m at an angle of 75°;
- An interface curve with a length of 50 m;
- A straight line with a length of 100 m.

Figure 1 shows the definition of the test traveling path, the traveled distance and speed of the model wagon in time, and the schematics of wagon's movement and different views of the test path.

2.2.2. Wagon modeling

A wagon of the "Plur e Sabz" type train with bogies of MD523 type is modeled for the simulation with the same characteristics of the wagon for which the experimental data are recorded. The wagon consists of many components whose geometrical and mechanical properties should be modeled for wagon-rail dynamic simulations. The wagon components can be subdivided into: (1) body components that hold the wagon mass (weight) including the wagon's body, wheelsets, and bogie frames; (2) suspension components including various physical springs and dampers such as traction rods, antiroll bars, bump stops, linkages, trailing arms, etc. [33]. The model of detailed components of wagon is created by the simulation software. This model consists of sixty-six degrees of freedom. The mass of all of the components is concentrated at the center of gravity of the wagon and their flexibilities are ignored. The friction model used for the dynamic friction force between the various surfaces such as pads (between

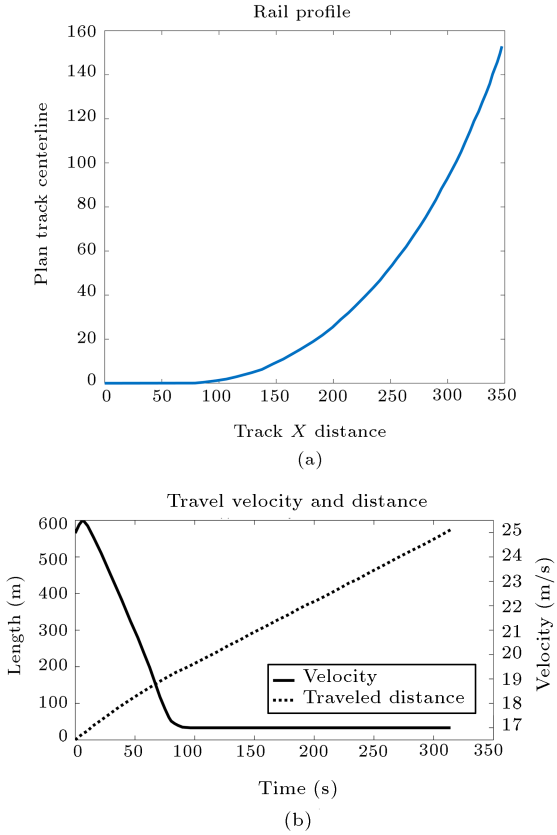

Figure 1. (a) The traveling path definition in software. (b) The travelled distance and speed of the model wagon in time.

body and bolster) is defined by a friction coefficient as a function of speed and compressive force of the contact surfaces.

A bogie is a set of mechanical parts including wheels and axles, suspension system, brake system, and bogie frame. Each wagon consists of two bogies; thus, each bogie bears half of the weight of the wagon. Obviously, when a wagon brakes or creates acceleration or deceleration or is in ascending or descending slopes, or in curves, the load that each bogie bears is more than its static loadings at rest. In general, several factors including the speed of the train and the radius of the curve are considered for the design of the bogie. The general geometrical parameters of the bogie and wagon are listed in Tables 2 and 3. The modeled bogie and wagon are shown in Figure 2.

2.2.3. Wheelsets and rail

The wheelsets consist mainly of the axles and wheels. Each axle connects rigidly two wheels. The wheel on each axle has a conical shape. The flange of a wheel is its inner edge, which is designed to prevent the derailment of the wagon during the travel, especially in curves. The wheel geometry is such that if any small lateral movements occur when the wagon travelling through the rail path, a centripetal force toward

Table 2. General characteristics of model bogie MD523.

Description	Value (mm)
Wheel gauge	1500
Rail gauge	1435
Distance between primary springs	2000
Distance between secondary springs	2580
Distance between side bearers	1410
Distance between pivots	19000
Wheel base	2500
Primary suspension spring play	32
Secondary suspension spring play	80

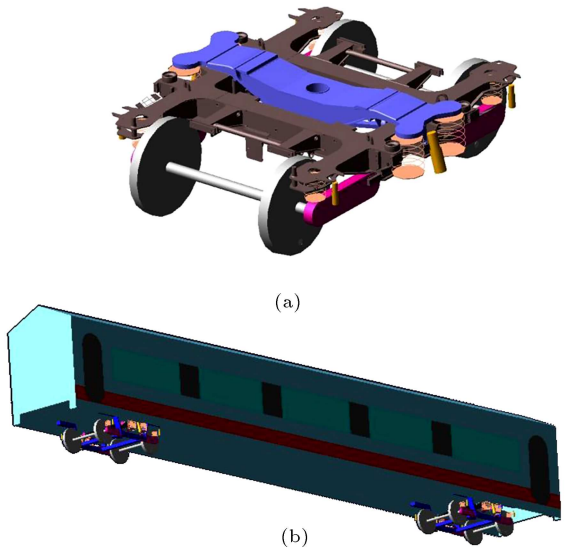

(a)

(b)

Figure 2. The models of (a) bogie of type MD523 and (b) the wagon of type Plure Sabz, in the simulation software.

the center of the wheel and axle returns the wagon to its initial position and compensates the produced temporal deviation. Moreover, the implementation of the restoring force can increase the radial consistency of the wheelset in curves. This consistency can increase the rolling and decrease the sliding of the wheels and, hence, can decrease the wheel and rail wear phenomenon resulting from the sliding of the wheels on the rail. The gap between the wheel and rail cannot exceed a specific limit either in the straight line or curved tracks (Figure 3(b)). This specific limit constrains the lateral movements. To model the wheel/rail contact in the software, the given wheel and rail profiles must be defined. UIC60 profiles are applied to rails and wheels; new and worn profiles of standard S1002 are used. Figure 3 represents the characteristics of the wheelset and rail in contact, the wheel and rail profiles and their definition in the software, and the naming convention of the wheels and bogies.

2.2.4. The wheel/rail contact problem

Since the 1960s, much research has been dedicated to the fundamental issues of the wheel/rail contact problem, because the characteristics of the wheel/rail contact mainly affect the dynamic interaction between vehicle and track. Hertz [34,35] used the early elastic theories that were related particularly to the calculation of surface tractions of wheel/rail in a track. He presented the contact surface formula as a prediction of an ellipse by calculating its small and large diameters. Finally, Hertz analytically calculated the force and stress at the contact point or on the contact surface with simplified assumptions presented as follows:

1. The contact surfaces are flat;
2. The contact between the bodies is frictionless;
3. The contact is assumed to be elliptic;
4. The important dimensions of the contact region are very small with respect to the dimensions of the bodies in contact.

In general, the creep forces are created at the contact of two rolling bodies, which are not considered in Hertz Contact Theory. When the two bodies are compressed to each other and are then rolled by a given force due to the difference between their strain rates at the contact point, some forces are created in the contact region. These forces are non-conservative and may cause the instability of the dynamic system. In addition, these forces depend on factors such as environmental conditions, surface smoothness, and the material and geometry of the wheel and rail. The creep motions mainly occur in the curved paths to define a deviation from the pure rolling motion. In particular, the difference between the lengths of inner and outer rails in a curve makes the two wheels in an axle of the wagon produce creep motions, hence producing wheel wear.

Table 3. The geometry of the passenger wagon model.

Description	Value (m, kg)
Car body (SGP)	Mass: 370000 Ixx: 7.5E+04 Iyy: 2.06E+06 Izz: 2.06E+06
	Body length: 26 body height: 3.42 body width: 3.0
	Graphic vertical offset: −1.1 CM location: 0, 0, −0.59
Distance between pivot center	Distance: 19
Hard point	0, 0, −1.1

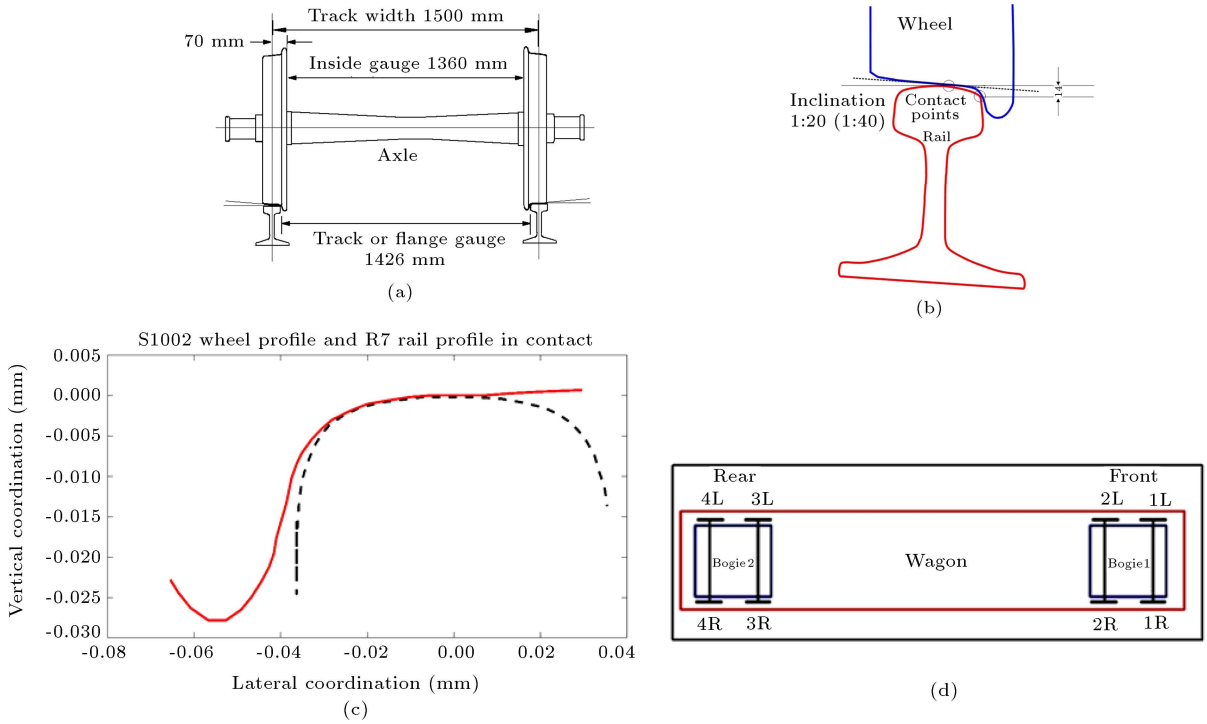

Figure 3. (a) The characteristics of wheel and rail on rail with a gauge of 1435 mm. (b) Wheel and rail profiles with their balance contact position. (c) The defined wheel and rail profiles in the software. (d) The naming convention of the wheels and bogies.

In 1967, Kalker [36] suggested a linear theory to illustrate that, for the creep, the slip zone is too small to have a considerable effect and, hence, its effect might be negligible. Therefore, it could be assumed that the sticky area represents the contact region. In this theory, a constant normal load could be assumed in the straight line; however, the influence of the contact of the wheel flange on the distribution of normal load in curves should be included. The linear theory of Kalker for the rail vehicles is widely used in the calculation of lateral stability and steady state forces in curves. Kalker formulated two nonlinear creep laws including the effects of rotational creep in his later works [37]. These two laws are added to the simple theory of rolling contact. The difference between the solutions originates from the two simplified assumptions, which are related to the tangential stress of the displacement and the distribution of the normal stress in the contact region. Kalker's theory [37] produces the best results of deviation from the pure rolling motion.

The linear theory of Kalker is used for the wheel/rail contact in our simulations. In this analysis, a multi-point connection model is used for the contact of the wheel and rail. In a multi-point contact, the analysis procedure is based on the non-linear polynomial equations due to the full consideration of the profile of the wheel/rail contact. The contact type is modeled based on the existing standards, which have been prescribed in geometrical tables.

2.2.5. The forces acting on the wheel and rail in contact

Specifying the forces between wheel and rail in their contact region is one of the most important issues related to the dynamics of train motion. The mutual effects between a track and vehicle are determined based on these forces. The forces acting on the wheel and rail are divided into tangential and normal forces acting on the contact surface. In the contact forces between the wheel and rail, the created stresses may lead to the transition of the material behavior from the elastic mode to the plastic mode. Tangential forces are the main reasons for the wheel damages such as wear and fatigue. Figure 4 shows the schematics of the longitudinal and translational radii of curvature and the distribution of the longitudinal and translational forces.

The design of the railroad tracks and wheels is based on the specifications and orientation of the vehicle in the track line (Rail). In a curve, both of the radii of the curvature and the effect of centripetal forces specify the characteristics of the contact between the wheel and rail. Centripetal forces cause the lateral compressing forces of the wheel on the outer rail. The centripetal forces depend on the vehicle mass, the radius of curvature, and the vehicle speed. The wear in the rail/wheel contact depends on the friction force in the contact region. The friction force depends on the coefficient of friction and the compressive normal

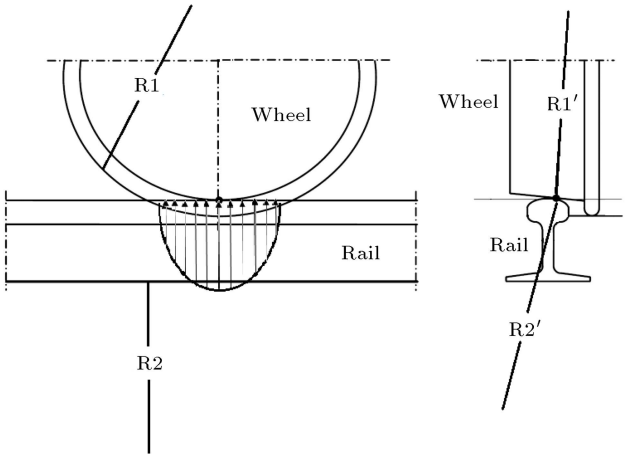

Figure 4. The schematics of the longitudinal and translational radii of curvature and the distribution of the longitudinal and translational forces.

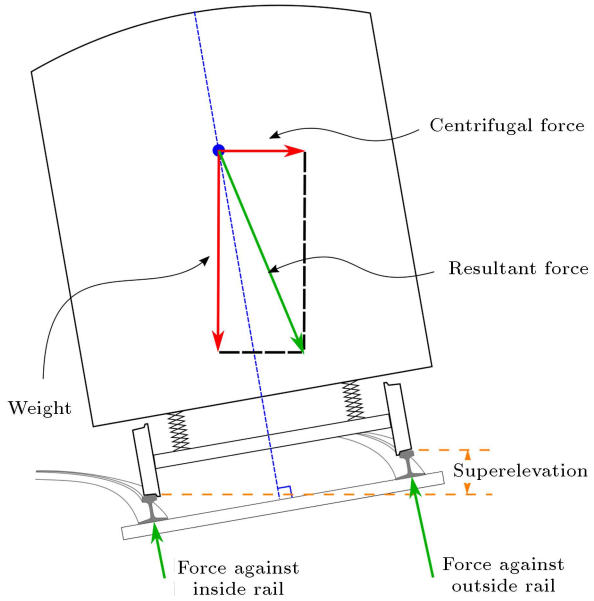

Figure 5. The wheel and axle set in curve with a lateral slope and the acting forces. Derailment occurs due to lateral forces acting on the wagon in curves.

forces. To reduce friction, it is beneficial to reduce the impact of each of these two factors. Lubrication is used to reduce the friction coefficient, and the transverse slope is used to reduce the normal compressive forces. The forces are shown in Figure 5.

The centripetal force and weight of the wagon along the line AA' acting on the wheel yield:

$$\sum f_{AA'} = m\frac{V^2}{R} \times \cos(\alpha) - mg \times \sin(\alpha), \tag{1}$$

where α is the transverse slope of the track line, g is the acceleration of gravity, V is the vehicle speed, R is the radius of curvature, and m is the mass of the vehicle.

If there is no transverse slope of the track line, $\sum f_{AA'}$ (the resultant of the forces acting on the wheels) is presented by:

$$\sum f_{AA'} = m \times \frac{V^2}{R}. \tag{2}$$

If the transverse slope increases, the resultant force acting on the wheel decreases. The ideal condition is satisfied when the magnitude of this force is zero. This occurs when the angle takes the following value:

$$\alpha = \tan^{-1}\left(\frac{V^2}{Rg}\right). \tag{3}$$

2.2.6. The wear index

As presented in the previous sections, creep forces (deviation from the pure rolling motion) are produced in the contact region between two rotating objects (wheel and rail). These non-conservative forces depend on the following factors: (1) environmental conditions, (2) surface smoothness of rotating objects, (3) materials of rotating objects, and (4) geometry of rotating objects. The dimensionless parameter, creep, is defined along the longitudinal and transverse directions with ζ_x and ζ_y, respectively. The equation of the wear index is then defined as follows:

$$\text{Wear index} = F_x \times \zeta_y + F_y \times \zeta_x, \tag{4}$$

where, from this definition, the dimension of the wear index is the same as the dimension of force.

2.2.7. Effect of wear on derailment

The flange on the inner edge of the wheel prevents the derailment of the wagon during the motions and its deviations from the lateral forces in curves, etc. Figure 6 shows a diagram of forces acting on the wheel flange when passing through a curve. In this condition,

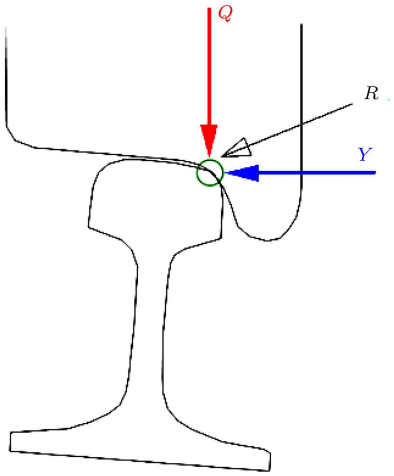

Figure 6. The resultant of the forces acting on the wheel flange. Q is the vertical force, Y is the lateral force, and R is the resultant force.

the wheel deviates from its balanced position and its flange creates one or more contact points with the rail edge. According to Figure 6, the lateral force, Y, and the vertical force, Q, are the components of the resultant force, R, acting on the wheel flange. The parameter causing the derailment is force Q, producing the lifting force for the wheel. Therefore, in wheel and its flange design, attempts are made to reduce the ratio (Y (lateral force))/(Q (normal force)), which is called " derailment ratio" [38]. In the worst cases, the components of the exerted forces are large enough to overcome the friction force and the wheel moves relative to the rail. $(Y/Q)_{\text{limit}}$ is the maximum allowable amount of Y/Q in the safe mode. Practically, the limit of Y/Q is achieved experimentally. By approaching the amount of Y/Q to $(Y/Q)_{\text{limit}}$, the probability of the derailment increases.

2.2.8. Transient solution

In order to carry out wear analysis and software simulation, the time step size or the number of the time divisions should be chosen small enough to obtain the desirable results when applying different profiles. If time is greater than the required amount, the obtained answers will not be sufficiently accurate. The time step size must also be chosen in such a way that the results would converge. For this purpose, the time step is set by using a trial-and-error procedure.

3. Results and discussions

The model of wagon and the path is created, and the simulations of the wheel profiles measured from the field data of the real wagon in service traveling through the Southern line of Iran are carried out. In the next step, the dynamic analysis of the curved path based on the given speed is the same as data measurement conditions, and the effects of wear of wheel profiles on the dynamic behavior of the wagon are considered with respect to the derailment ratio and wear index.

3.1. Experimental data

The wagon sweeps along the Southern line of Iran's railway system with a length of 905 km. The wheels' profile data are recorded for each round trip (1810 km). Seven worn profiles are selected for the simulations. These wheel profiles represent the history of the severe flange wear from 32 mm for a new profile to the minimum of 22 mm for the last worn profile. This limit has been defined in the standard UIC510-2 for the detachment of the wheel in order to repair the worn wheel or replace it with a new wheel. After traveling about 40,000 km, the wheel number 1L (called "critical wheel") is detached due to severe wear in the flange thickness (Sd) of 22.9 mm. Figure 6 represents the new and worn profiles, which are defined in the software for the purpose of conducting simulations [3]. The technique of curve fitting is used to model the wear procedure of the critical wheel. Figure 7 represents the 1st- to 5th-order polynomial functions that fit with the experimental data of flange thickness; the evaluation of the parameters shows that, among them, the 5th-order polynomial function is the best fitted model [3].

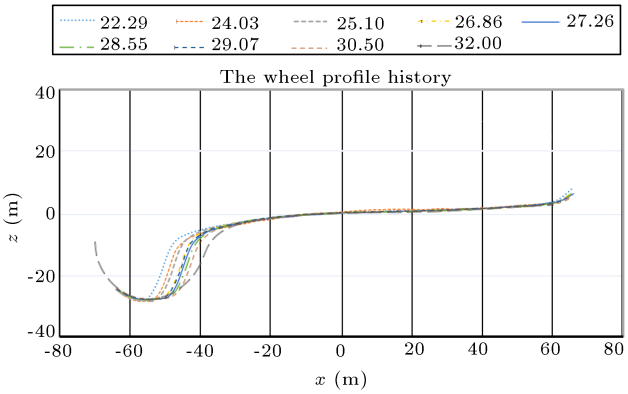

Figure 7. The experimental data of the selected worn profiles obtained from field measurements [3].

3.2. The derailment analysis

One of the outputs of the dynamic analysis in the dynamic simulation software is the safety analysis related to the derailment by the lateral and vertical forces between wheel and rail. The derailment ratio must be smaller than 0.8 according to the standard UIC-518. Here, the critical derailment ratio is only considered for the critical wheel.

3.2.1. Derailment ratio

According to Figure 1(b), by a steep variation in the wagon speed in time $t = 6$ s (which is the state in which the wagon passes through the first transient distance (interface curve) from a length 100 m to a length 150 m), the corresponding peaks for the new and selected worn profiles of the critical wheel can be observed (Figure 8). Figure 9 shows the history of the peak derailment ratio through the worn profiles of the critical wheel. Therefore, it is found that by increasing the amount of wear of the profiles, the derailment ratio increases. However, according to UIC518, it must not exceed the limit of 0.8. The results show that the derailment ratio is always less than this limit in our simulations. Hence, the derailment does not occur for the wheels of this wagon through the prescribed path and test conditions.

The plot of the peak derailment ratio (Figure 9) can be divided into three zones. The first zone (28 mm $< Sd <$ 32 mm) (shows that the flange thickness wear is relatively small in this region. In this zone, the lateral forces increase continuously with respect to the vertical forces. The amount of wheel flange thickness (Sd) for the detachment of the critical wheel for repair or replacement is not efficient in this zone.

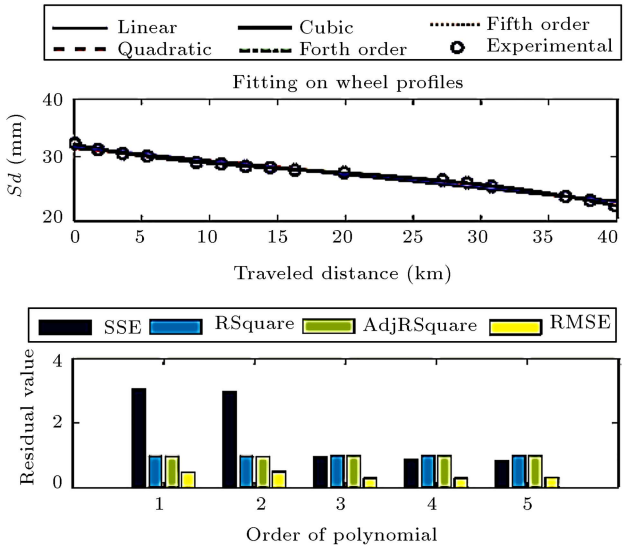

Figure 8. (a) The fitting evaluation parameters in order to choose the best fitted model. (b) 1st to 5th order polynomial functions fitted to the experimental data of flange thickness versus the travelled distance [3].

However, in the second zone, the range of wheel flange thickness is 25 mm $< Sd <$ 28 mm, and the plot shows local minimums with respect to the third zone in the range of 22 mm $< Sd <$ 25 mm. In the third zone, a continuously increasing trend can be observed for the derailment ratio, which can greatly increase the risk of derailment.

3.2.2. Wear index

Similar to the derailment ratio, according to Figure 10, the wear index plots show corresponding peaks in their plots for the new and worn profiles of the critical wheel (1L). Figure 11 shows the variation of the peak wear index of the critical wheel. It is found that by increasing the amount of wear in the profiles, the wear index increases, but not for all the range. Figure 12 represents the zone 25 mm $< Sd <$ 27 mm, where the wear index is minimum. This range can be used in maintenance strategies to optimize the maintenance costs and schedules.

Based on the wear index and derailment ratio from the dynamic analysis, an appropriate range of the wheel flange thickness for repairing or replacement of the worn wheel is suggested to be 25 mm $< Sd <$ 27 mm.

4. Conclusion

In this paper, the experimental data were recorded from the field measurements of the worn wheels of a passenger wagon in the Southern line of Iran's railway system and were combined with the dynamic simulations in the software to study the dynamic behavior of the wagon by two parameters: wear index and derailment ratio. The wheels' profile data recorded for

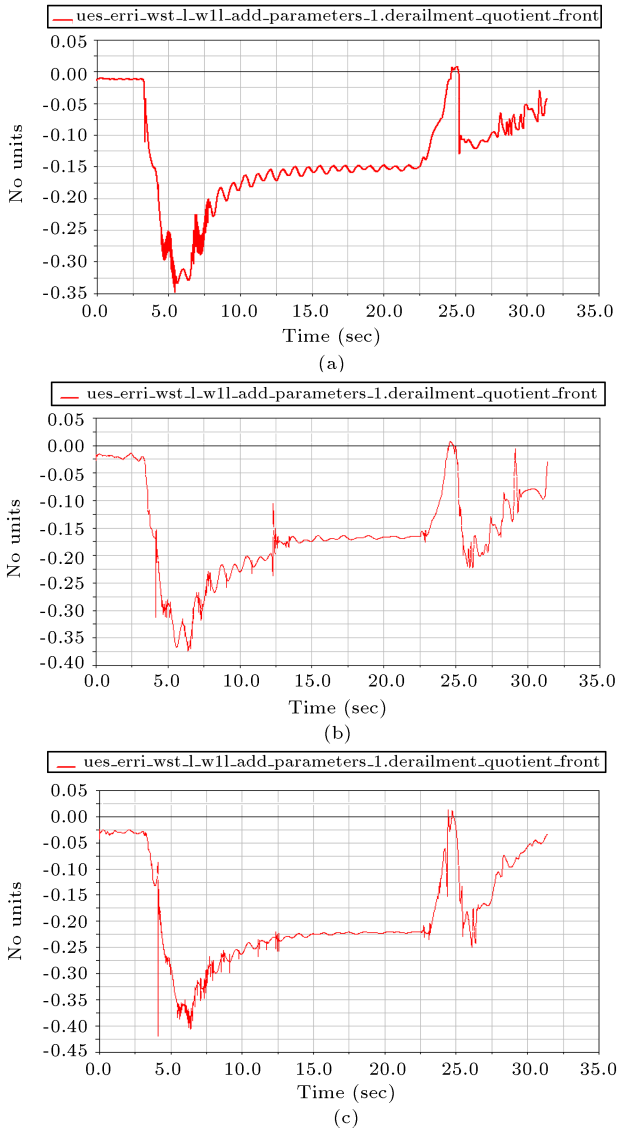

Figure 9. The derailment ratio of the (a) new, (b) first worn, and (c) last worn, profiles of the critical wheel (1L). The derailment ratio shows corresponding peaks for the new and worn profiles.

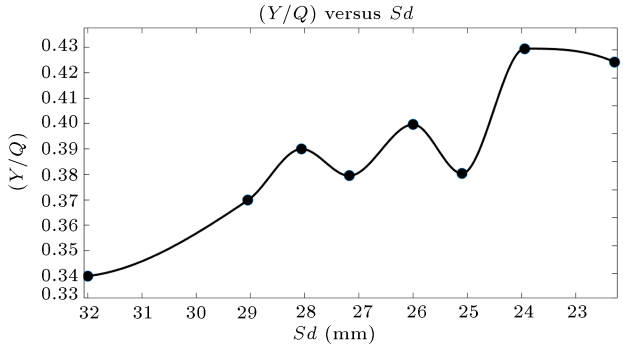

Figure 10. The peak derailment ratio variation for the critical wheel (1L). There are three zones with respect to the wheel flange thickness (Sd). The minimum peak derailment ratio occurs in flange thickness range 25 mm $< Sd <$ 28 mm.

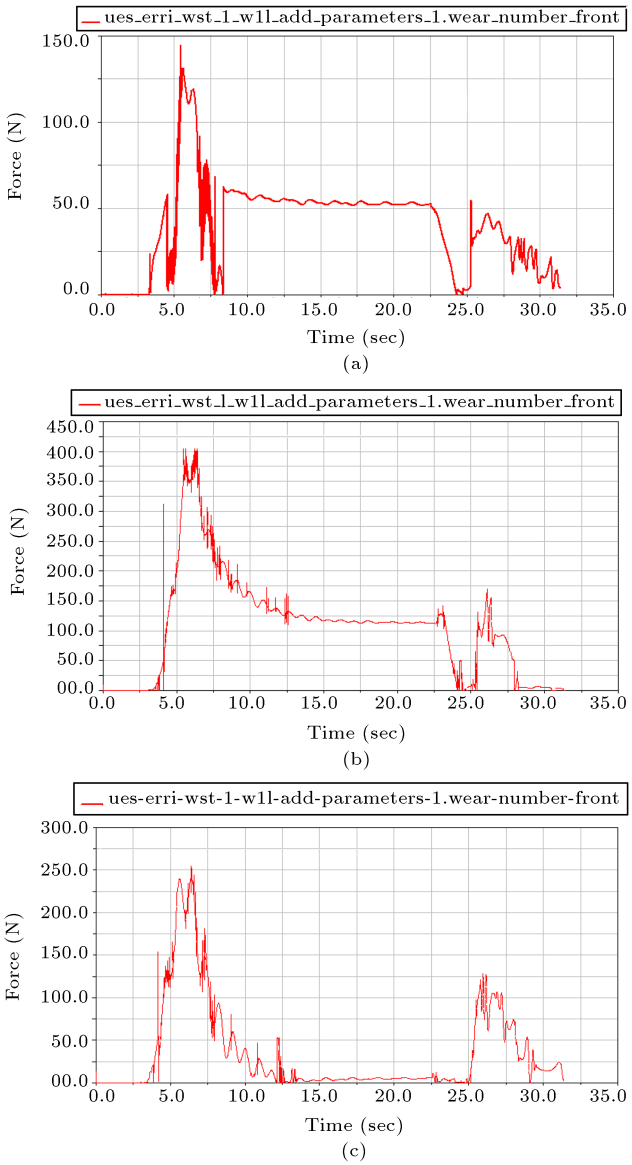

Figure 11. The wear index for the (a) new, (b) first worn, and (c) last worn, profiles of the critical wheel (1L). The wear index shows corresponding peaks for the new and worn profiles.

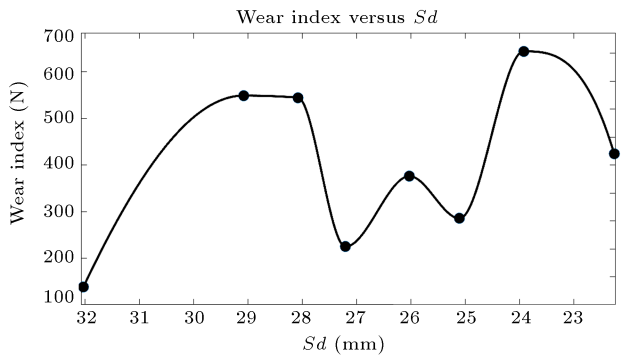

Figure 12. The wear index of the critical wheel (1L) versus wheel flange thickness (Sd). It represents the minimum zone of the wear index for the range of wheel flange thickness 25 mm $< Sd <$ 27 mm.

each round trip and seven worn profiles of the critical wheel (the first wheel detached due to the wear) were selected for further consideration. The technique of curve fitting was used to model the wear procedure of the critical wheel. The evaluation of parameters showed that the 5th-order polynomial equation was the best fitted model.

The results of the variations of the derailment ratio and wear index of the wheel profiles with respect to the wheel flange thickness (Sd) during the traveling of the train showed that the amount of wheel wear directly impacted the dynamic behavior of the wagon in curves. In general, an increase in the amount of wear in profiles increased the derailment ratio. It was found that the derailment ratio for the tests is always below the limit of 0.8 according to standard UIC518, where exceeding the limit increases the hazard of the derailment of the wagon. However, when wheel wear is in a certain range, the wear index and derailment ratio are reduced. The appropriate range of the wheel flange thicknesses for repairing or replacement of the worn wheel is suggested to be 25 to 27 mm.

References

1. Knothe, K. and Stichel, S. "Modeling of wheel/rail contact", In *Rail Vehicle Dynamics*, Springer, pp. 33-79 (2017).

2. Höjer, M., Bergseth, E., Olofsson, U., Nilsson, R., and Lyu, Y. "A noise related track maintenance tool for severe wear detection of wheel-rail contact", *Civil-Comp Proceedings*, **110**, p. 146 (2016).

3. Salehi, S.M., Farrahi, G.H., and Sohrabpoor, S. "A study on the contact ellipse and the contact pressure during the wheel wear through passing the tracks including several sharp curves", *International Journal of Engineering*, **31**(5), pp. 795-803 (2018).

4. Zhai, W., Gao, J., Liu, P., and Wang, K. "Reducing rail side wear on heavy-haul railway curves based on wheel-rail dynamic interaction", *Vehicle System Dynamics*, **52**(sup1), pp. 440-454 (2014).

5. Shebani, A. and Iwnicki, S. "Prediction of wheel and rail wear under different contact conditions using artificial neural networks", *Wear*, **406**, pp. 173-184 (2018).

6. Wei, L., Zeng, J., Wu, P., and Gao, H. "Indirect method for wheel-rail force measurement and derailment evaluation", *Vehicle System Dynamics*, **52**(12), pp. 1622-1641 (2014).

7. Meymand, S.Z., Keylin, A., and Ahmadian, M. "A survey of wheel-rail contact models for rail vehicles", *Vehicle System Dynamics*, **54**(3), pp. 386-428 (2016).

8. Lewis, R. and Olofsson, U., *Wheel-Rail Interface Handbook*, Elsevier (2009).

9. Sheinman, E. "Wear of rails. A review of the American press", *Journal of Friction and Wear*, **33**(4), pp. 308-314 (2012).

10. Wang, W., Guo, J., and Liu, Q. "Experimental study on wear and spalling behaviors of railway wheel", *Chinese Journal of Mechanical Engineering*, **26**(6), pp. 1243-1249 (2013).

11. Wang, W.-J., W.-J. Jiang, H.-Y. Wang, Q.-Y. Liu, M.-H. Zhu, and X.-S. Jin "Experimental study on the wear and damage behavior of different wheel/rail materials", *Proceedings of the Institution of Mechanical Engineers, Part F: Journal of Rail and Rapid Transit*, **230**(1), pp. 3-14 (2016).

12. Naeimi, M., Li, Z., and Dollevoet, R.P.B.J. "Scaling strategy of a new experimental rig for wheel-rail contact", *International Journal of Mechanical, Aerospace, Industrial, and Mechatronics Engineering*, **8**(12) (2014).

13. Askarinejad, H., Dhanasekar, M., Boyd, P., and Taylor, R. "Field measurement of wheel-rail impact force at insulated rail joint", *Experimental Techniques*, **39**(5), pp. 61-69 (2015).

14. Jin, X. "Experimental and numerical modal analyses of high-speed train wheelsets", *Proceedings of the Institution of Mechanical Engineers*, Part F: *Journal of Rail and Rapid Transit*, **230**(3), pp. 643-661 (2016).

15. Baharom, M. "Experimental prediction of wear rate on rail and wheel materials at dry sliding contact", *MATEC Web of Conferences*, **13**, p. 03013 (2014).

16. Daves, W., Kubin, W., Scheriau, S., and Pletz, M. "A finite element model to simulate the physical mechanisms of wear and crack initiation in wheel/rail contact", *Wear*, **366**, pp. 78-83 (2016).

17. Tao, G., Wen, Z., Zhao, X., and Jin, X. "Effects of wheel-rail contact modelling on wheel wear simulation", *Wear*, **366**, pp. 146-156 (2016).

18. Sharma, S.K., Sharma, R.C., Kumar, A., and Palli, S. "Challenges in rail vehicle-track modeling and simulation", *International Journal of Vehicle Structures & Systems*, **7**(1), pp. 1-9 (2015).

19. Alarcón, G.I., Burgelman, N., Meza, J.M., Toro, A., and Li, Z. "The influence of rail lubrication on energy dissipation in the wheel/rail contact: A comparison of simulation results with field measurements", *Wear*, **330**, pp. 533-539 (2015).

20. Dirks, B. *Simulation and Measurement of Wheel on Rail Fatigue and Wear*, KTH Royal Institute of Technology (2015).

21. Moreno-Ríos, M., Gallardo-Hernández, E.A., Vite-Torres, M., and Peña-Bautista, A. "Field and laboratory assessments of the friction coefficient at a railhead", *Proceedings of the Institution of Mechanical Engineers*, Part F: *Journal of Rail and Rapid Transit*, **230**(1), pp. 313-320 (2016).

22. Zhou, Y., Wang, S., Wang, T., Xu, Y., and Li, Z. "Field and laboratory investigation of the relationship between rail head check and wear in a heavy-haul railway", *Wear*, **315**(1-2), pp. 68-77 (2014).

23. Sharma, S.K. and Kumar, A. "Dynamics analysis of wheel rail contact using FEA", *Procedia Engineering*, **144**, pp. 1119-1128 (2016).

24. Peng, D., Jones, R., Constable, T., Lingamanaik, S., and Chen, B. "The tool for assessing the damage tolerance of railway wheel under service conditions", *Theoretical and Applied Fracture Mechanics*, **57**(1), pp. 1-13 (2012).

25. Bogacz, R., Czyczuła, W., and Konowrocki, R. "Effect of periodicity of railway track and wheel-rail interaction on wheelset-track dynamics", *Archive of Applied Mechanics*, **85**(9-10) pp. 1321-1330 (2015).

26. Iwnicki, S., *The Manchester Benchmarks for Rail Vehicle Simulation*, Routledge (2017).

27. Maya-Johnson, S., Santa, J.F., and Toro, A. "Dry and lubricated wear of rail steel under rolling contact fatigue-wear mechanisms and crack growth", *Wear*, **380**, pp. 240-250 (2017).

28. Kalker, Joost J., *Three-Dimensional Elastic Bodies in Rolling Contact*, Springer Science & Business Media, **2** (2013).

29. Zhao, X. and Li, Z. "A three-dimensional finite element solution of frictional wheel-rail rolling contact in elasto-plasticity", *Proceedings of the Institution of Mechanical Engineers*, Part J: *Journal of Engineering Tribology*, **229**(1) pp. 86-100 (2015).

30. Meymand, S.Z. "State of the art roller rig for precise evaluation of wheel-rail contact mechanics and dynamics", Doctoral Dissertation, Virginia Tech University (2016).

31. Salehi, S., Farrahi, G., and Sohrabpour, S. "A new technique of the 'first and second limits' for wagon maintenance in railway tracks consisting of sharp curves based on the empirical study of wheel wear", *Scientia Iranica, Transaction B, Mechanical Engineering*, **24**(3) p. 1171 (2017).

32. UIC "UIC 510-2: Trailing stock: Wheels and wheelsets, conditions concern", International Union of Railways (2004).

33. Iwnicki, S., *Handbook of Railway Vehicle Dynamics*, CRC press (2006).

34. Hertz, H. "On contact between elastic bodies", *Reine Angew Math*, **92**, pp. 156-171 (1881).

35. Hertz, H. "On the contact of elastic solids", Z. Reine Angew, *Mathematik*, **92**, pp. 156-171 (1881).

36. Kalker, J.J. "On the rolling contact of two elastic bodies in the presence of dry friction", *TU Delft*, Delft University of Technology (1967).

37. Kalker, J. "Wheel-rail rolling contact theory", *Wear*, **144**(1), pp. 243-261 (1991).

38. Iwnicki, S. "Simulation of wheel-rail contact forces", *Fatigue & Fracture of Engineering Materials & Structures*, **26**(10), pp. 887-900 (2003).

39. UIC "UIC 513: Guidelines for evaluating passenger comfort in relation to vibration in railway", International Union of Railways (2005).

Biographies

Seyyed Miad Salehi received his PhD degree in Mechanical Engineering in 2016 from Sharif University of Technology in Tehran. He has received several national and international awards and prizes in his various activities such as the nation's leading student in 2012 and Kharazmi Young Award in 2007 and 2012.

Gholam Hossein Farrahi received his PhD degree in Mechanical Engineering in 1985 from (ENSAM), Paris, France. He is currently Professor at the School of Mechanical Engineering, Sharif University of Technology. He is also the Head of Materials Life Assessment and Improvement Laboratory. His research interests include structural integrity assessment, failure analysis, fatigue, wear and life improvement methods.

Saeed Sohrabpour received his PhD degree in Mechanical Engineering in 1971 from University of California, Berkeley, USA. His research interests include large deformations, mechanics of metal forming, and optimal design.